Anesthesiology
66:168-175, 1987

Relationship Between Invasive and Noninvasive Measurements of Gas Exchange in Anesthetized Infants and Children

Sten G. E. Lindahl, M.D., Ph.D., Alan P. Yates, M.B.B.S., F.F.A.R.C.S.,† David J. Hatch, M.B.B.S., F.F.A.R.C.S.**

Minute ventilation ($\dot{V}_E$), tidal volume (V_T), carbon dioxide elimination ($\dot{V}_{CO_2}$), and end-tidal ($P_{ET}CO_2$) and arterial CO_2 tensions (Pa_{CO_2}) were measured in 39 anesthetized infants and children with body weights ranging from 3.1 to 31 kg. Eighteen children had normal cardiopulmonary function, seven had acyanotic congenital heart disease, and 11 had cyanotic congenital heart disease. One child had left heart failure and pulmonary congestion, and two had severe parenchymal lung disease. To evaluate differences between pulmonary gas exchange calculated from Pa_{CO_2} *versus* $P_{ET}CO_2$, dead space volume (V_D) and alveolar ventilation ($\dot{V}_A$) based on a Pa_{CO_2} (V_Da, $\dot{V}_A$a) as well as on $P_{ET}CO_2$ (V_DET, $\dot{V}_A$ET) were performed, and correlations between $Pa_{CO_2} - P_{ET}CO_2$, V_Da/V_T − V_DET/V_T, and $\dot{V}_A$a − $\dot{V}_A$ET were carried out. It was demonstrated that in normal children, as well as in those with acyanotic congenital heart disease, $P_{ET}CO_2$ correlated closely with Pa_{CO_2} (r = 0.94, 0.98, respectively). In children with cyanotic congenital heart disease, however, correlation between $P_{ET}CO_2$ and Pa_{CO_2} was relatively poor (r = 0.61). Mean values for Pa_{CO_2} were significantly higher than $P_{ET}CO_2$ in the cyanotic children ($P < 0.01$), resulting in significant underestimation of physiologic dead space ($P < 0.05$) and significant overestimation of alveolar ventilation ($P < 0.01$). In three patients with pulmonary disease, large differences between Pa_{CO_2} and $P_{ET}CO_2$ were comparable with those observed in the children with cyanotic congenital heart disease. It is concluded that in normal children and in children with acyanotic heart disease during anesthesia, noninvasive measurement of $P_{ET}CO_2$ can be used as a reliable estimate of Pa_{CO_2} and for calculations of physiologic dead space and alveolar ventilation. In children with cyanotic congenital heart disease and severe pulmonary disease, $P_{ET}CO_2$ does not provide a precise estimate of Pa_{CO_2}, and calculations of physiologic dead space and alveolar ventilation should be based on direct measurements of Pa_{CO_2}. (Key words: Equipment: CO_2 analyzer; pneumotachograph. Heart: acyanotic heart disease; congenital heart disease; cyanotic heart disease. Lung: alveolar ventilation; dead space; gas exchange; mechanical ventilation.)

THE CO_2 GRADIENT between alveolar gas and blood leaving pulmonary capillaries is small, and because "ideal" alveolar gas is contaminated by alveolar dead space gas, the CO_2 tension in arterial blood has been substituted for the "ideal" alveolar CO_2 tension in calculations of gas exchange.[1-5] Peripheral arterial samples, however, reflect the results of total lung perfusion, including blood perfusing "ideal" alveoli as well as that perfusing alveoli distal to closed airways and anatomic arteriovenous shunts. Noninvasive pulmonary gas analysis and evaluation of gas exchange based on end-tidal CO_2 analysis are becoming more frequently used in clinical anesthesia.[6,7] The accuracy of estimates of gas exchange without the use of arterial blood samples needs to be evaluated, especially in infants and children. In the child, apparatus dead space assumes relatively greater importance than in adults because the absolute volume of physiologic dead space is smaller. Apparatus dead space, therefore, may lead to rebreathing of carbon dioxide and elevated end-tidal CO_2 values. Furthermore, abnormal lung perfusion also changes ventilation–perfusion ratios, which could make the end-tidal CO_2 tension into a poor estimate of the arterial CO_2 tension. This might jeopardize noninvasive calculations of alveolar ventilation and dead space volume and ought to be elucidated.

To evaluate differences between pulmonary gas exchange calculated from arterial *versus* end-tidal CO_2 tension, we measured ventilation and concomitant arterial and end-tidal CO_2 tension in anesthetized infants and children with normal as well as abnormal lung perfusion and lung function.

Patients and Methods

Thirty-nine children between 1 month to 9 yr of age and with body weights ranging from 3.1 to 31 kg were investigated. All patients were fasted for at least 4 to 5 h before induction of anesthesia. The patients were divided into four groups with regard to their cardiopulmonary function and symptoms. Patient data are presented in table 1. The study was approved by the Hospital Ethical Committee.

Children with a normal physical examination of heart and lungs, a clear chest x-ray, hemoglobin (Hb) between 10 and 15 $g \cdot dl^{-1}$, and hematocrit (Hct) < 45% comprised the *normal* group, which consisted of 18 patients (ASA P.S. I) subjected to thoracic or neurosurgical operative procedures. In one case, embolization of a facial hem-

* Consultant Anaesthetist.

† Senior Registrar.

Received from the Department of Anaesthesia, Hospital for Sick Children, London, United Kingdom. Accepted for publication September 16, 1986. Supported by grants from the Medical Faculty, University of Lund, Sweden, The Wenner-Gren Foundations, Stockholm, Sweden, and the Swedish Medical Research Council, Stockholm (Project No. B86-19X-007189-02A).

Dr. Lindahl's current address is: Department of Anesthesiology, Mayo Clinic, Rochester, Minnesota 55905.

Dr. Yates's current address is: Department of Anaesthesia, University College Hospital, Gower Street, London WC1E 6JA, United Kingdom.

Address reprint requests to Dr. Lindahl.

TABLE 1. Patient Data

Patient No.	Age (yr/month)	Body Weight (kg)	Diagnosis	Operations	Hemoglobin ($g \cdot dl^{-1}$)	Hematocrit (%)	Symbol*
Normal patients							
1	0/8	5.5	Coarctation of aorta	Repair	11.1	34.0	○
2	6/5	18.7	Posterior fossa tumor	Exploration—excision	13.4	41.7	○
3	1/4	7.9	Posterior fossa tumor	Exploration—excision	11.5	36.7	○
4	7/9	23.3	Coarctation of aorta	Correction	12.9	40.7	○
5	0/2	4.6	Sagittal suture synostosis	Craniotomy	9.9	31.4	○
6	9/2	31	Hemangioma—cheek	Embolization	13.2	41.8	○
7	5/9	17.8	Craniopharyngeoma	Craniotomy	9.3	30.0	○
8	5/3	19.5	Pineal tumor	Exploration—excision	11.1	36.3	○
9	0/5	5.2	Morgagni diaphragmatic hernia	Correction	14.2	45.5	○
10	0/4	6.8	Bilateral coronal suture synostosis	Craniotomy	10.5	32.1	○
11	5/6	21	Spinal cord glioma	Laminectomy	12.6	40.2	○
12	0/4	4.6	Coarctation of aorta	Repair	10.5	32.4	○
13	0/5	4.7	Cloacal abnormality	Correction	8.9	29.5	○
13	1/0	9.6	Bilateral coronal suture synostosis	Craniotomy	11.3	36.3	○
15	4/7	20	Optic nerve glioma	Craniotomy	12.0	36.8	○
16	4/2	16.6	Pectus excavatum	Correction	12.9	38.8	○
17	3/5	14.9	Cervical dermoid diastema	Laminectomy	10.7	33.0	○
18	0/7	5.7	Coarctation of aorta	Correction	12.9	38.3	○
Acyanotic heart disease							
19	2/2	12.9	VSD	Closure	12.9	40.3	□
20	0/9	5.2	VSD	Closure	11.0	33.7	□
21	0/4	4.2	VSD	Closure	10.4	32.0	□
22	4/1	14.9	Fallot	Correction	13.9	41.0	□
23	2/3	8.2	Acyanotic Fallot	Correction	12.6	42.0	□
24	5/1	16.9	A–V canal (Down's syndrome)	Correction	12.5	37.8	□
25	0/1	3.1	Transposition, large PDA, small VSD	Sennings' procedure	11.9	36.2	
Cyanotic heart disease							
26	4/2	15.7	Tricuspid stresia, pulmonary stenosis	Fontans' procedure	17.7	60.2	●
27	5/1	15.6	VSD, pulmonary stenosis	Closure, conduit	15.4	49.2	●
28	0/4	5.8	Transposition of great vessels	Sennings' procedure	16.3	52.9	●
29	6/3	16.4	Fallots' anomaly, interrupted aortic arch	Correction	14.7	47.0	●
30	3/8	10.3	VSD, interrupted aortic arch	Correction	16.2	55.3	●
31	2/2	10.5	Fallot's anomaly (Down's syndrome)	Correction	16.3	53.1	●
32	0/8	7.2	Transposition of great vessels	Sennings' procedure	19.0	58.8	●
33	0/3	4.2	Total anomalous pulmonary venous drainage	Correction	15.9	46.9	●
34	1/0	6.9	Fallot's anomaly	Correction	14.5	46.8	●
35	5/7	14.3	Pulmonary atresia, multiple pulmonary collaterals	Mobilization of collaterals	16.3	48.7	●
36	5/7	14.3	Pulmonary atresia, multiple pulmonary collaterals	Closure of collaterals, conduit	16.3	48.7	●
Pulmonary disease							
37	0/8	7.0	Aortic stenosis, pulmonary congestion	Open valvotomy	10.8	34.7	△
38	0/2	6.6	Pneumonia, upper lobe consolidation	—	13.7	42	△
39	3/7	12.6	Interstitial pneumonitis	—	12.6	38.9	△

Patients 6, 10, 11, 14, 15, and 17 were studied during spontaneous respiration. Patients 35 and 36 are the same patients studied at different occasions under different conditons.

VSD = ventricular septal defect; PDA = patent ductus arteriosus.
* The different symbols are used to identify the patients in figures 3–5.

angioma was performed. Based on physical examination of heart and lungs, cardiac catheterizations, and echocardiography, 18 other patients with congenital heart disease were classified as acyanotic (n = 7, ASA P.S. II) if a normal or overperfused lung existed and Hb and Hct were normal; and as *cyanotic* (n = 11, ASA P.S. II) if peripheral cyanosis was present, lung perfusion was normal or oligemic, and Hb and Hct were increased. Three patients were classified as having pulmonary disease. One child (patient 37, table 1) with severe aortic stenosis and left heart failure had high end-diastolic left ventricular pressures, raised left atrial pressure, and pulmonary congestion. Two children (patients 38 and 39, table 1) were both being mechanically ventilated in the intensive care unit (ICU) for respiratory failure due to pneumonitis. In children scheduled for surgery, measurements were performed prior to the start of operation.

PREMEDICATION

Patients with body weights less than 10 kg were premedicated with atropine 0.2–0.3 mg im. Patients not sub-

TABLE 2. Mean Values (±SEM) for Systolic Blood Pressure and Heart Rate in the Three Groups

	Systolic Blood Pressure (mmHg)	Heart Rate (beats/min)
Normal n = 18	101 ± 3	122 ± 6
Acyanotic n = 7	103 ± 7	143 ± 6
Cyanotic n = 11	105 ± 6	129 ± 5

jected to intracranial surgery received premedication that included an opioid analgesic. Children weighing between 10 and 15 kg received meperidine compound 0.07 $ml \cdot kg^{-1}$ (1 ml contains meperidine 25 mg, promethazine 6.25 mg, and chlorpromazine 6.25 mg) and atropine 1 h before induction of anesthesia. Children heavier than 15 kg received Omnopon® 0.4 $mg \cdot kg^{-1}$ and scopolamine 0.008 $mg \cdot kg^{-1}$ im 90 min prior to anesthesia. Children undergoing intracranial operations were premedicated with atropine 0.2–0.4 mg im and dexamethasone. Patients 38 and 39 were not premedicated. They were both studied under light diazepam sedation in the ICU.

ANESTHESIA

Anesthesia was induced with cyclopropane in oxygen (fraction of inspired O_2 [FI_{O_2}] 0.5). The trachea was intubated in all patients after the injection of succinylcholine 1–1.5 $mg \cdot kg^{-1}$ iv. Those patients who were allowed to resume spontaneous respiration breathed through a Mapleson F system with fresh gas flows of O_2 in N_2O (FI_{O_2} 0.5) and halothane 0.75–1%. The fresh gas flow was set high enough to avoid rebreathing, as indicated by stable zero inspired carbon dioxide tension during inspiration (shown by the capnometer). In the remainder, anesthesia was maintained with O_2/N_2O (FI_{O_2} 0.5) and halothane 0.50–1%, with muscle relaxation achieved by tubocurarine 0.4 $mg \cdot kg^{-1}$. Six children in the normal group were breathing spontaneously. In all others, ventilation was mechanically controlled with an Engstrom ventilator 2000 set at an inspiration/expiration (I/E) ratio of 1:2 and with a rate between 20 and 30 cycles per min, with the higher rates in younger patients.

MEASURING APPARATUS

An in-line infrared capnometer (Hewlett-Packard, 14360A) and a pneumotachograph (Fleisch no. 00 or Fleisch no. 0) were placed in the apparatus dead space, with airway pressures being measured at the endotracheal tube connection. The dead space of the system was 6 ml with the Fleisch no. 00 and 8 ml with the Fleisch no. 0 measured by water displacement. The inspiratory and expiratory resistances of the measuring apparatus were 16 $cmH_2O \cdot l^{-1} \cdot s^{-1}$ for the Fleisch no. 00 and 18 $cmH_2O \cdot l^{-1} \cdot s^{-1}$ for the Fleisch no. 0 at a flow rate of 8 $l \cdot min^{-1}$. No measurements were made until the inspired halothane concentration and the level of anesthesia were stable and at least 20 min had elapsed since induction. All measurements were performed prior to surgery.

Minute ventilation ($\dot{V}_E$) was measured by electrical integration of the flow signal from the heated pneumotachograph and a differential pressure manometer (Validyne, MP 45-1-871, range ± 2 cmH_2O). The highest flow rate in the sample was 15 $l \cdot min^{-1}$ measured in patient 27. The Fleisch no. 00 used in patients below 8 kg in body weight was linear for flow rates up to 8 $l \cdot min^{-1}$ and the Fleisch no. 0, used in the heavier patients, up to flow rates of 16 $l \cdot min^{-1}$. The capnometer was positioned at the tube connection followed by the heated pneumotachograph; it had a response time of 0.05 s, and a well-identified end-tidal plateau was reached in all patients. Airway

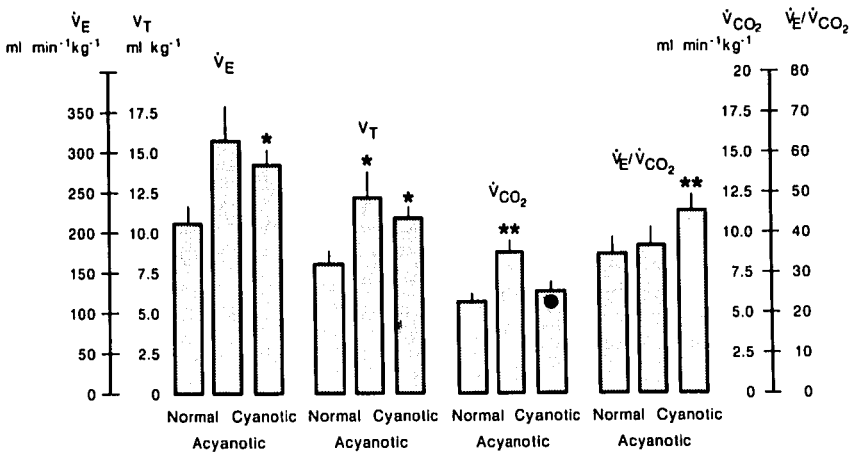

FIG. 1. Mean values (±SEM) of minute ventilation ($\dot{V}_E$), tidal volume (V_T), CO_2 output ($\dot{V}_{CO_2}$), and $\dot{V}_E/\dot{V}_{CO_2}$ ratios in the three groups. * = $P < 0.05$ and * * = $P < 0.01$ for differences between the normal group and acyanotic as well as cyanotic groups. • = $P < 0.05$ for the difference between cyanotic and acyanotic groups.

TABLE 3. Mean Values (±SEM) of Hemoglobin, Hematocrit, *p*H, Pa_{O_2}, Pa_{CO_2}, and Standard Bicarbonate (HCO_3^-) in the Three Groups

	Hemoglobin ($g \cdot dl^{-1}$)	Hematocrit (%)	*p*H	Pa_{O_2} (mmHg)	Pa_{CO_2} mmHg	HCO_3^- $mmol \cdot l^{-1}$
Normal n = 8	11.6 ± 0.4	36.4 ± 1.1	7.39 ± 0.02	201.8 ± 12.8	37.1 ± 2.1	22.4 ± 0.7
Acyanotic n = 7	12.2 ± 0.4	37.8 ± 1.4	7.41 ± 0.03	149.3 ± 27.8	30.5 ± 2.8	19.6 ± 1.6
Cyanotic n = 11	16.2 ± 0.4	51.6 ± 1.5	7.35 ± 0.02	57.8 ± 6.0	34.7 ± 1.9	20.6 ± 0.7

The statistically significant differences between normal and cyanotic groups as well as between acyanotic and cyanotic groups were for hemoglobin ($P < 0.001$), hematocrit ($P < 0.001$), *p*H ($P < 0.05$), and Pa_{O_2} ($P < 0.01$).

The differences of Pa_{O_2} and Pa_{CO_2} between the normal and acyanotic groups were also statistically significant ($P < 0.05$).

pressure was measured by a Druck® transducer (PDCR-75). Flow, volume, airway pressure, and end-tidal CO_2 tension (PET_{CO_2}) were recorded on an inkjet recorder (Siemens-Elema, EM 81).

Expired gas passed to a dry gas meter (Standard gas meter, AB Nordgas, Stockholm, Sweden) and then to a three-way valve from which a timed collection, over 5 min, could be made into a Douglas bag. The mean exhaled fraction of CO_2 ($F\bar{E}_{CO_2}$) in the bag was then immediately measured by the capnometer. Arterial blood (0.5 ml) was sampled in heparinized syringes and analyzed within 3 min in a conventional blood gas machine (Corning 168), which was calibrated twice daily and found to be stable between the two calibrations. Corrections for body temperature were made.

$\dot{V}_E$, alveolar ventilation ($\dot{V}_A$), tidal volume (V_T), dead space volume (V_D), dead space minute volume ($\dot{V}_D$), and carbon dioxide elimination ($\dot{V}_{CO_2}$) were corrected to body temperature and pressure saturated (BTPS). Body temperature varied between 36.5 to 37.3° C in the study.

CALIBRATION

Flow and volume were calibrated with an accurate pump that delivered a flow of 50 $ml \cdot s^{-1}$ and a volume of 30 ml. Flow from the pump was checked against a precision rotameter and the volume against a super syringe. Accuracy and precision of the pump was tested by repeated measurements on a wet gas meter. The reliability of repeated measurements of flow from the pump was within ±0.5%. Readings of flow and volume were corrected for viscosity changes caused by temperature and nitrous oxide. The capnometer was calibrated with a certified gas of 5.51% CO_2 (gas mixture prepared gravimetrically after actual weight and percentage were determined by gas chromotography). Carbon dioxide calibrations were also carried out by the use of the calibration device on the capnometer giving 58.1 mmHg. Calibration of the capnometer showed linearity within this range of CO_2. Due to collision broadening of the infrared spectrum, corrections of the CO_2 signal for the presence of

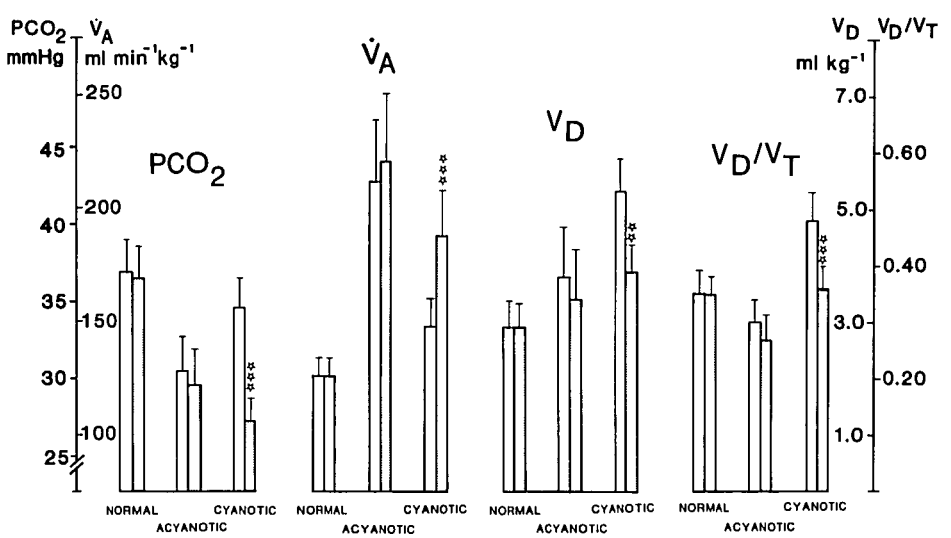

FIG. 2. Mean values (±SEM) of $Pa_{CO_2} - PET_{CO_2}$, $\dot{V}_A a - \dot{V}_A ET$, $V_D a - V_D ET$, and $V_D a/V_T - V_D ET/V_T$ in normal (n = 18), acyanotic (n = 7), and cyanotic (n = 11) children. *Open columns* represent Pa_{CO_2} or values calculated from Pa_{CO_2} tensions, while *hatched columns* represent PET_{CO_2} or values calculated from PET_{CO_2} tensions. ✡✡ = $P < 0.01$ and ✡✡✡ = $P < 0.001$ for differences between arterial and end-tidal values.

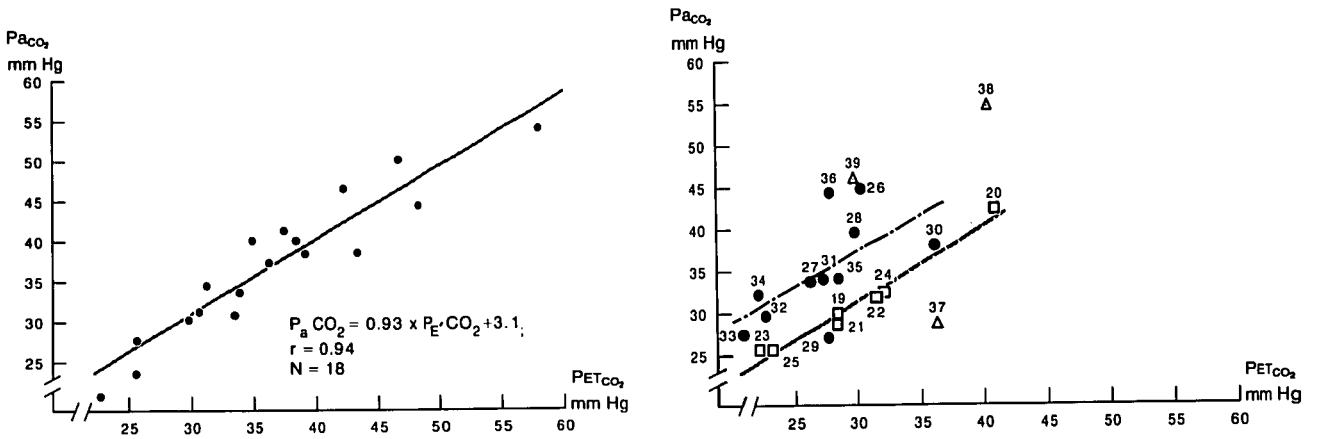

FIG. 3. Relationships between Pa_{CO_2} and PET_{CO_2}. In the normal group (*left*), the regression line is drawn and the standard error of the estimate is shaded. The normal standard error of the estimate is shaded and individual relationships between Pa_{CO_2} and PET_{CO_2} are shown for acyanotic (*squares*, – – – = regression line) and for cyanotic patients (*filled circles* –·–·– = regression line) (*right*). The difference between slopes of regression lines in acyanotic and cyanotic patients was statistically significant ($P < 0.01$). △ and ▲ indicate patients with pulmonary disease. Individuals may be identified from the numbers (see table 1). Regression equations are presented in table 4.

N_2O and 50% oxygen were done. The pressure transducer was calibrated at a negative pressure of −20 cmH_2O.

STATISTICS

Mean values, SD, and SEM were calculated. Linear regressions were performed and between-group comparisons were carried out with paired and unpaired one- and two-tailed *t* tests. Probability values below 0.05 were considered to indicate statistical significance.

TABLE 4. Regression Equations and Coefficients of Correlations for the Relationships between Pa_{CO_2} and PET_{CO_2}, $\dot{V}_Aa$ and $\dot{V}_AET$, and V_Da/V_T and V_DET/V_T

Group	Regression Equation	Coefficient of Correlation (r)
n = 18 Normal	Pa_{CO_2} (mmHg) = 0.93 PET_{CO_2} + 3.1	0.94
	$\dot{V}_Aa$ (ml/min) = 1.0 $\dot{V}_AET$ − 21.4	0.98
	V_Da/V_T = 1.10 V_DET/V_T − 0.03	0.95
n = 7 Acyanotic	Pa_{CO_2} (mmHg) = 0.90 PET_{CO_2} + 3.9	0.98
	$\dot{V}_Aa$ (ml/min) = 0.92 $\dot{V}_AET$ + 67.7	0.99
	V_Da/V_T = 0.89 V_DET/V_T + 0.06	0.95
n = 11 Cyanotic	Pa_{CO_2} (mmHg) = 0.85 PET_{CO_2} + 11.4	0.60
	$\dot{V}_Aa$ (ml/min) = 0.95 $\dot{V}_AET$ − 289	0.92
	V_Da/V_T = 1.20 V_DET/V_T + 0.05	0.92

See text for abbreviations.

Results

Systolic blood pressure and heart rate (mean ± SEM) were similar in the normal, acyanotic, and cyanotic groups (table 2). Mean values (±SEM) of $\dot{V}_E$, V_T, $\dot{V}_{CO_2}$, and the $\dot{V}_E/\dot{V}_{CO_2}$ ratios are presented in figure 1 for all three groups. Pa_{O_2} was normal or higher than normal in the normal and acyanotic groups but low in the cyanotic group (table 3). This group also had a low *p*H and high Hb and Hct (table 1). The Pa_{CO_2} (mean) was somewhat higher in the normal than in the acyanotic group ($P < 0.05$, table 3).

ARTERIAL AND END-TIDAL CO_2 TENSIONS

The difference between mean values of Pa_{CO_2} and PET_{CO_2} was only 0.45 mmHg in the normal and 0.98 mmHg in the acyanotic group. The six spontaneously breathing children in the normal group had a Pa_{CO_2} (mean ± SEM) of 43.1 ± 2.0 mmHg and a PET_{CO_2} (mean ± SEM) of 43.2 ± 1.7 mmHg. In the cyanotic group the difference between mean values of Pa_{CO_2} and PET_{CO_2} was 7.5 mmHg ($P < 0.001$, fig. 2), with an average (±SEM) Pa_{CO_2} of 34.7 ± 1.9 mmHg and PET_{CO_2} 27.2 ± 1.4 mmHg. The patient with pulmonary congestion (patient 37, table 1) had a PET_{CO_2} that was 8.2 mmHg higher than the Pa_{CO_2}, while patients 38 and 39 with parenchymal lung disease had PET_{CO_2}s that were 14.0 and 14.9 mmHg lower than corresponding Pa_{CO_2}s.

The significant correlation between Pa_{CO_2} and PET_{CO_2} (r = 0.94) in the normal group is defined in fig. 3*A* and table 4. The range of the $P(a-ET)_{CO_2}$ difference was from −5.3 to +5.3 mmHg in the normal group, with

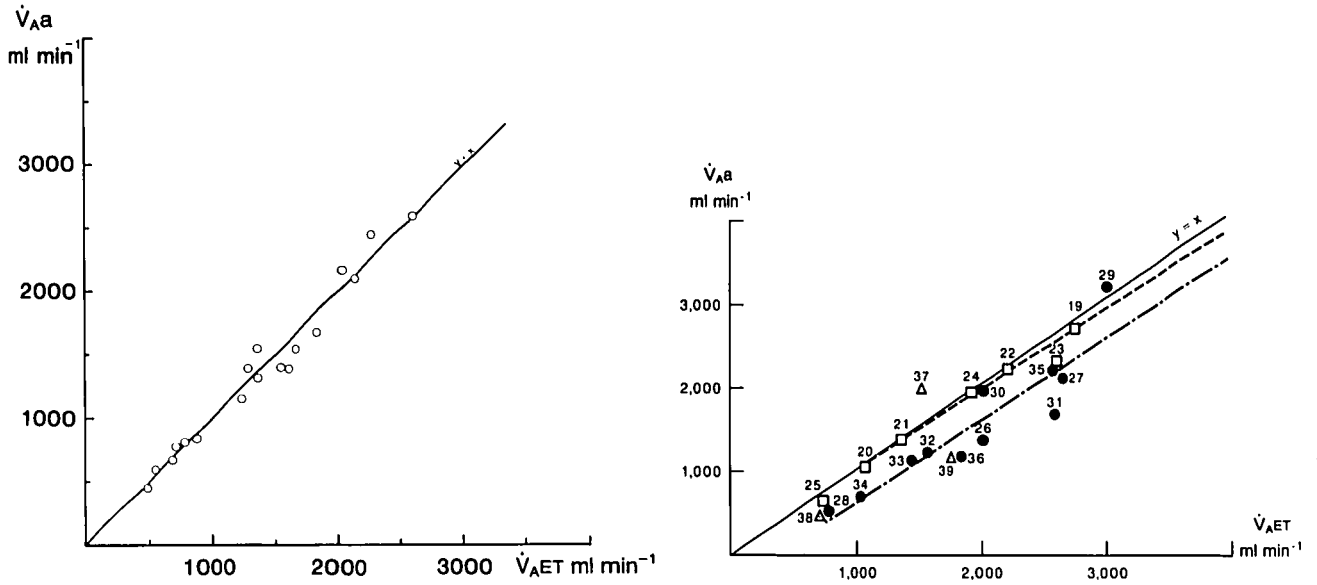

FIG. 4. Correlations between $\dot{V}_A a$ and $\dot{V}_A ET$ in the normal group (*left*) (*open symbols*, line of identity is drawn) as well as in the acyanotic (*left*) (*open squares*, – – – = regression line) and cyanotic (*right*) (*filled circles*, –·–·– = regression line) children. The continuous line represents the line of identity between $\dot{V}_A a$ and $\dot{V}_A ET$. The difference between slopes of regression lines for acyanotic and cyanotic patients was statistically significant ($P < 0.05$). △ and ◬ indicate patients with pulmonary disease. Numbers are given for individual identification in table 1. Regression equations are presented in table 4.

PET_{CO_2} being higher than Pa_{CO_2} in six cases. Of these, two were breathing spontaneously. All patients in the acyanotic group (n = 7) had a $P(a-ET)_{CO_2}$ difference within the standard error of the estimate for the normal group (fig. 3*B*). In the cyanotic group, only two patients had a $P(a-ET)_{CO_2}$ difference within this range (fig. 3*B*). All other children in the cyanotic group and the three patients with pulmonary disease had larger differences (fig. 3*B*).

Alveolar Ventilation

There was no difference between mean values of $\dot{V}_A a$ and $\dot{V}_A ET$ in the normal group (fig. 2) and the relationship between the two is shown in fig. 4*A* and table 4. The difference between mean values of $\dot{V}_A a$ and $\dot{V}_A ET$ was only 4% in acyanotic patients, while cyanotic patients had a difference of 27% ($P < 0.001$, fig. 4*B*) as a consequence of the difference in arterial and end-tidal CO_2 tension measurements. Regression equations and coefficients of correlation are presented in table 4. In the patients with pulmonary disease, the differences between $\dot{V}_A a$ and $\dot{V}_A ET$ exceeded 25% (fig. 4*B*).

Dead Space and V_D/V_T Ratio

In the normal and acyanotic groups mean $V_D a$ and $V_D ET$ were virtually identical, while $V_D ET$ in the cyanotic group was 26% lower than $V_D a$ ($P < 0.01$, fig. 2), as would be expected from differences in Pa_{CO_2} and PET_{CO_2}.

Similarly, the differences between $V_D a/V_T$ and $V_D ET/V_T$ in the normal and acyanotic groups were small, while a 25% difference was found in the cyanotic patients (*P*

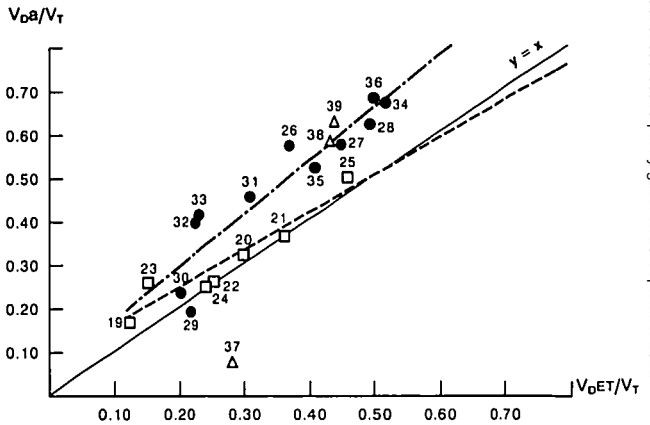

FIG. 5. The line of identity between $V_D a/V_T$ and $V_D ET/V_T$ ratios is represented by the continuous line. The correlations for each individual in the acyanotic (*open squares*, – – – = regression line) and cyanotic (*filled circles*, –·–·– = regression line) groups are presented. The difference between slopes of regression lines for acyanotic and cyanotic patients was statistically significant ($P < 0.01$). △ and ◬ indicate patients with pulmonary disease. Individuals are identified in table 1, and regression equations given in table 4.

TABLE 5. Comparison of Pa_{CO_2} Calculations According to the Regression Equation PET_{CO_2} (kPa) = 0.81 × Pa_{CO_2} + 0.83; r = 0.80, published by Lindahl *et al.*[8] and the Regression Equation Found in This Study for the Normal Group

Measured PET_{CO_2} (mmHg)	Calculated Pa_{CO_2} (mmHg)	
	This Study	Lindahl *et al.*[8]
22.5	24	20.3
30	31	29.3
37.5	40	39
45	45	48

Values from Lindahl *et al.* are converted from kPa to mmHg.

< 0.001, fig. 2). Individual values of patients in the acyanotic and cyanotic groups are presented in fig. 5. Regression equations and coefficients of correlation are presented in table 4.

Discussion

Acyanotic patients with normal hematology and arterial oxygen tensions showed a high correlation between arterial and end-tidal CO_2 tensions (fig. 3), which agrees with previously published data in children.[8,9] This was not the case, however, in the cyanotic group of patients in whom the $P(a-ET)_{CO_2}$ difference was large, and only two patients had a relation between arterial and end-tidal CO_2 tensions that fell within the normal range (fig. 3). This is most probably explained by the greater dead space volumes in this group (fig. 2), which during exhalation diminishes alveolar CO_2 tension and results in end-tidal CO_2 tensions that are lower than arterial CO_2 tensions. The child who had a left heart failure with pulmonary congestion (patient 37) demonstrated, on the other hand, a higher PET_{CO_2} than Pa_{CO_2} (fig. 3B). One reason for a higher PET_{CO_2} could be that pulmonary congestion, *i.e.*, an increased pulmonary blood volume, causes an alveolar CO_2 tension closer to venous than to arterial. The relationship between pulmonary blood volume, arterial, venous, and end-tidal CO_2 tensions ought, however, to be further elucidated.

With the exception of the patients with pulmonary disease, it was in the cyanotic group that the large $P(a-ET)_{CO_2}$ differences existed. The mean difference of arterial to end-tidal CO_2 tension gradient of 27% resulted in an alveolar ventilation that was 27% higher and in a V_D/V_T ratio that was 25% lower when calculated from end-tidal rather than arterial CO_2 tensions (fig. 2). This illustrates the limitations of gas exchange calculated from noninvasive end-tidal CO_2 tensions in those patients with longstanding oligemic pulmonary circulation due to congenital malformations. Large $P(a-ET)_{CO_2}$ differences related to abnormal lung perfusion have previously been published by Heneghan *et al.*[10] based on measurements before and during pulmonary artery occlusion. This was also stated in an experimental study by Julian *et al.*[11] where pulmonary artery occlusion in dogs was performed to decrease pulmonary blood flow abruptly. Furthermore, the present study agreed with previous results[12] that severe parenchymal lung disease increases ventilation–perfusion inequalities, and accordingly the $P(a-ET)_{CO_2}$ difference, which also adversely influences evaluations of alveolar ventilation and dead space volumes from end-tidal CO_2 measurements. The magnitude of the $P(a-ET)_{CO_2}$ difference can, however, be of clinical use, for instance, in the monitoring of improvement after operative corrections of low lung perfusion[13] as well as in clinical evaluation of patients with severe lung disorders who are artificially ventilated in the ICU. Accordingly, we and others[5] think that it is important to state whether calculations are based on arterial or end-tidal P_{CO_2} when determining alveolar ventilation and dead space volumes.

In patients with normal cardiopulmonary function, as well as in those with cardiac malformations resulting in overperfusion of the lungs, the correlation between arterial and end-tidal CO_2 tensions was high and of about the same magnitude as previously published for children.[8,9] There was no difference between the $P(a-ET)_{CO_2}$ gradient in spontaneously breathing or in artificially ventilated children. If the regression equation found in this study (Pa_{CO_2} [mmHg] = 0.93 × PET_{CO_2} + 3.1) was used and the results from these calculations compared with those calculated from a formula published earlier,[8] deviations between measured PET_{CO_2} and calculated Pa_{CO_2} were small in both studies (table 5). We observed better correlation of end-tidal with arterial CO_2 tensions in our present study, in contrast to our previous study, because the capnometer currently employed had a much shorter response time.

Recently, doubt has been cast on noninvasive measurements of dead space based on PET_{CO_2} values (V_DET) because V_DET may show a large deviation from airway dead space (V_D^{aw}) when V_D^{aw} is calculated noninvasively from Fowler's method[14] using CO_2 as a tracer gas.[5] Our study indicates that measurements of dead space based on sampling of arterial P_{CO_2}, the best measure of true physiologic dead space (V_Dphys), can be closely estimated from accurate measurements of end-tidal P_{CO_2} (V_DET), a noninvasive method applicable to studies in normal children and those with uncomplicated, acyanotic congenital heart disease.

We conclude that end-tidal CO_2 tensions correlated closely with arterial CO_2 tensions in normal children (r = 0.94) as well as in children with acyanotic congenital heart disease (r = 0.98). This encourages the use of noninvasive measurements of gas exchange in anesthetized

children. In patients with cyanotic congenital heart disease, however, the end-tidal CO_2 will underestimate the arterial and, thus, lead to important underestimations of physiologic dead space and the V_D/V_T ratio and overestimations of alveolar ventilation.

References

1. Bohr C: Über die Lungenathmung. Skand Arch Physiol 2:236–269, 1891
2. Enghoff H: Volumen inefficax. Bemerkungen zur Frage des Schädlichen Raumes. Upsala Läkaref Förhand 44:191–218, 1938
3. Riley RL, Lilienthal JL Jr, Proemmel DD, Franke RE: On the determination of the physiologically effective pressures of oxygen and carbon dioxide in alveolar air. Am J Physiol 147: 191–198, 1946
4. Nunn JF: Applied Respiratory Physiology, 2nd edition. London, Butterworths, 1977, pp 214, 216
5. Fletcher R: Dead space, invasive and non-invasive. Br J Anaesth 57:245–249, 1985
6. Lindahl SGE, Hulse MG, Hatch DJ: Ventilation and gas exchange during anaesthesia and surgery in spontaneously breathing infants and children. Br J Anaesth 56:121–129, 1984
7. Hulse MG, Lindahl SGE, Hatch DJ: Comparison of ventilation and gas exchange in anaesthetized infants and children during spontaneous and artificial ventilation. Br J Anaesth 56:131–135, 1984
8. Lindahl S, Okmian L, Thomson D: Artificial ventilation in children during anaesthesia using a tidal volume ventilator. Acta Anaesthesiol Scand 23:587–595, 1979
9. Valentin N, Lomholt B, Thorup M: Arterial to end-tidal carbon dioxide tension difference in children under halothane anaesthesia. Can Anaesth Soc J 29:12–15, 1982
10. Heneghan CPH, Scallan MJH, Branthwaite MS: End-tidal carbon dioxide during thoracotomy: Its relation to blood level in adults and children. Anaesthesia 36:1017–1021, 1981
11. Julian DG, Travis DM, Robin ED, Crump CH: Effect of pulmonary artery occlusion upon end-tidal CO_2-tension. J Appl Physiol 15:89–91, 1960
12. Dumpit FM, Brady J: A simple technique for measuring alveolar CO_2 in infants. J Appl Physiol 4:648–653, 1978
13. Nicodemus HF, Downes JJ: Ventilatory alterations associated with operation for tetralogy of Fallot. ANESTHESIOLOGY 31:265–271, 1969
14. Fowler WS: Lung function studies. II. The respiratory dead space. Am J Physiol 154:405–416, 1948

APPENDIX

The following formulas were used in the article:

$$\dot{V}_{CO_2}(ml \cdot min^{-1}) = \text{gas collection } \dot{V}_E \times F\bar{E}_{CO_2};$$

$$\dot{V}_A a = \frac{\dot{V}_{CO_2} \times P_B}{Pa_{CO_2}}; \quad \dot{V}_A ET = \frac{\dot{V}_{CO_2} \times P_B}{PET_{CO_2}};$$

$$\dot{V}_D a = \dot{V}_E - \dot{V}_A a; \quad \dot{V}_D ET = \dot{V}_E - \dot{V}_A ET;$$

$$V_D a = \frac{\dot{V}_D a}{f}; \quad V_D ET = \frac{\dot{V}_D ET}{f};$$

where $\dot{V}_A a$, $\dot{V}_D a$, $V_D a$, and $\dot{V}_A ET$, $\dot{V}_D ET$, $V_D ET$ are alveolar ventilation and dead space calculated from arterial (a) and end-tidal (ET) CO_2 tensions, respectively. $\dot{V}_E$ is minute ventilation, respiratory rate is f, and $F\bar{E}_{CO_2}$ the mixed expired carbon dioxide fraction. P_B indicates atmospheric pressure. Pa_{CO_2} indicates arterial CO_2 tension and PET_{CO_2} is end-tidal CO_2 tension.